Journal of Organometallic Chemistry, 474 (1994) 165–171

Addition of some gold electrophiles to an octa-osmium carbonyl cluster: thermodynamic *vs.* kinetic control

Zareen Akhter, Scott L. Ingham, Jack Lewis and Paul R. Raithby

University Chemical Laboratory, Lensfield Road, Cambridge CB2 1EW (UK)

(Received October 21, 1993)

Abstract

The reaction of the dianionic cluster $[PPN]_2[Os_8(CO)_{22}]$ $\{[PPN]^+ = [N(PPh_3)_2]^+\}$ with Au_2Cl_2L {L = chelating phosphines *bis*-(diphenylphosphino)methane (dppm), 1,2-*bis*-(diphenylphosphino)ethane (dppe) or 1,4-*bis*-(diphenylphosphino)butane (dppb)} in the presence of an excess of the halide acceptor $TlPF_6$, affords the neutral digold-substituted clusters $[Os_8(CO)_{22}(Au_2L)]$ {(1) L = dppm; (2) L = dppe; (3) L = dppb} in almost quantitative yield. The $^{31}P\{^1H\}$ NMR spectra of these compounds indicate that the gold atoms are in non-equivalent environments and therefore cannot have a metal geometry similar to that previously reported for the related cluster $[Os_8(CO)_{22}(AuPPh_3)_2]$ (4). A reinvestigation of the reaction between $[PPN]_2$ $[Os_8(CO)_{22}]$ and monogold fragment '$AuPPh_3^+$' has shown that, in addition to (4), a second isomer of $[Os_8(CO)_{22}(AuPPh_3)_2]$ (5) is formed, which on the basis of the spectroscopic data is thought to have the same metal geometry as compounds (1–3). A single crystal X-ray diffraction study of the compound $[Os_8(CO)_{22}(Au_2dppb)]$ (3) has shown that the metal core consists of a bicapped octahedron of osmium atoms, with one of the gold atoms capping the osmium octahedron, and the other gold atom bridging an edge of the osmium core.

Key words: Osmium; Carbonyl; Cluster; Gold; Crystal structure

1. Introduction

Interest in high nuclearity carbonyl clusters has continued to develop [1–3] because they lie at the interface between conventional organometallic chemistry and the chemistry and physical properties of large metal particles. One of the most successful methods to date for synthesising high nuclearity hetero-bimetallic clusters has been the use of redox coupling reactions between preformed anionic carbonyl compounds and appropriate neutral or cationic mononuclear metal electrophiles [4–6]. The introduction of heterometallic metal–metal bonding into these clusters may lead to an increase in the polarity of the molecule, which in turn can result in enhanced electrochemical or photochemical reactivity [7].

We report here the reactions between the cluster $[PPN]_2[Os_8(CO)_{22}]$ and digold electrophiles of the type 'Au_2L^{2+}' {where L is a chelating phosphine} which gives neutral clusters with retention of the original osmium core geometry. This observation is in contrast to the results reported for the reaction between $[PPN]_2[Os_8(CO)_{22}]$ and the monogold electrophile '$AuPPh_3^+$', where a major rearrangement of the osmium core was observed [8]. Hence a reinvestigation of the reactivity between $[PPN]_2[Os_8(CO)_{22}]$ and the monogold electrophile '$AuPPh_3^+$' was undertaken and the results are presented.

2. Results and discussion

The dianionic cluster $[PPN]_2[Os_8(CO)_{22}]$ readily reacts in a dichloromethane solution with gold electrophiles of the type 'Au_2L^{2+}', {L = *bis*-(diphenylphosphino)methane (dppm), 1,2-*bis*-(diphenylphosphino)ethane (dppe) or 1,4-*bis*-(diphenylphosphino)-butane (dppb)}, to give a brown neutral cluster as the only product. These clusters have been formulated as $[Os_8(CO)_{22}(Au_2L)]$ {(1) L = dppm; (2) L = dppe; (3) L = dppb} on the basis of their spectroscopic and elemental data. The $^{31}P\{^1H\}$ NMR spectra of these compounds exhibit separate resonances attributable to each of the phosphorus nuclei, which indicate that the gold

---

Correspondence to: Dr. P.R. Raithby

0022-328X/94/$7.00
SSDI 0022-328X(93)24301-K

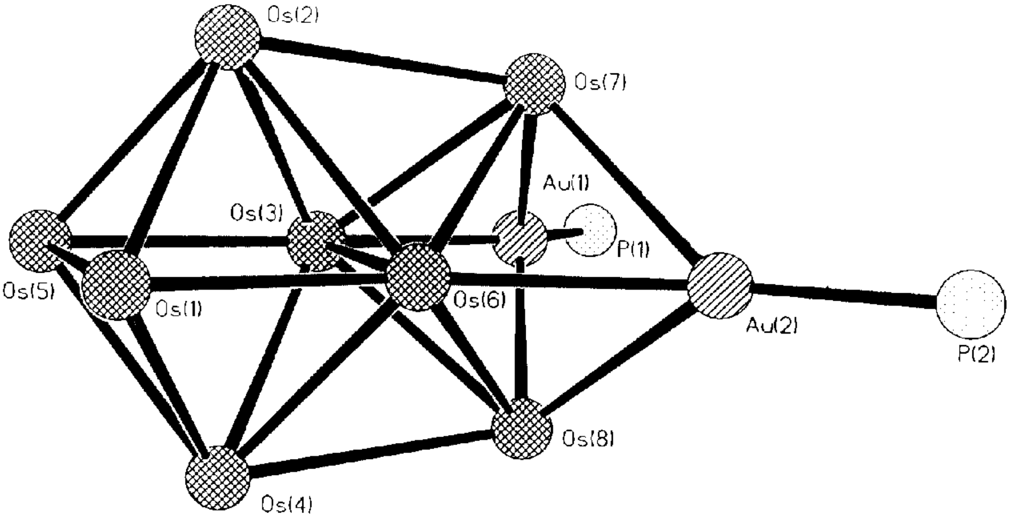

Fig. 1. Diagram depicting metal framework of previously reported isomer of $[Os_8(CO)_{22}(AuPPh_3)_2]$ (4).

atoms must coordinate to the metal core in non-equivalent sites. This observation is in contrast with that for the product **4** reported from the reaction of $[PPN]_2[Os_8(CO)_{22}]$ with the mono-gold fragment '$AuPPh_3^+$', where it has been shown that a major metal core rearrangement has occurred and the gold atoms are in equivalent sites (see Fig. 1). A reinvestigation of this latter reaction has shown that two products are formed from the reaction of $[PPN]_2[Os_8(CO)_{22}]$ with $AuPPh_3(NO)_3$, the first product being the previously

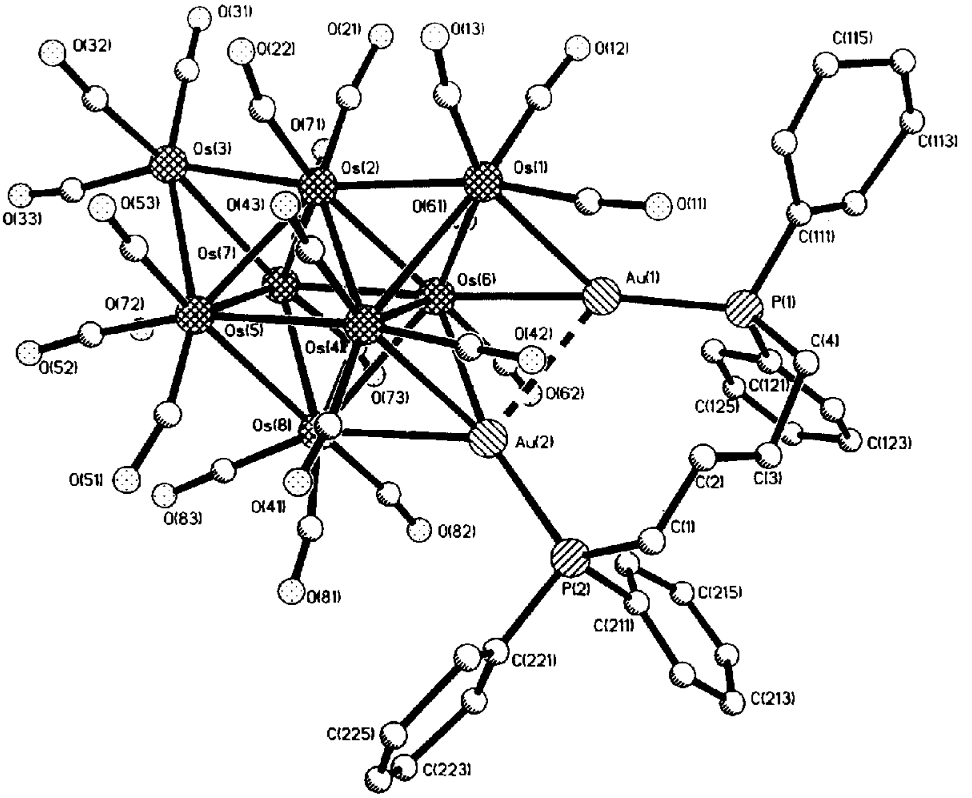

Fig. 2. Diagram depicting molecular structure of $[Os_8(CO)_{22}(Au_2dppb)]$ (3).

reported cluster **4**, whereas the second product has also been formulated as $[Os_8(CO)_{22}(AuPPh_3)_2]$ (**5**) on the basis of spectroscopic data and is formed initially as the major product from the reaction. This latter product, **5**, slowly converts to **4** upon standing in CH_2Cl_2 and hence with time **4** is the major product isolated from the reaction. It may therefore be considered as the thermodynamically favourable product, whereas the isomer **5** is the kinetically favoured product. On the basis of the spectroscopic data **5** is thought to have a same metal geometry as the clusters **–3**, however, no compounds were isolated that were analogous to **4** for the reactions with the digold electrophiles 'Au_2L^{2+}'. From this observation it seems feasible that the steric constraints of the chelating phosphine ligands do not allow the conversion of the products **1–3** to compounds that are analogous to **4**. The ${}^{31}P\{{}^1H\}$ NMR spectrum of **5** exhibits two resonances with very similar chemical shifts to the clusters **1–3**, whilst for the former product only one signal is observed and this supports the above formulation of the isomers of $[Os_8(CO)_{22}(AuPPh_3)_2]$. It is interesting to note that the metal framework of the clusters **1–3** and **5** appear to be stereochemically rigid in solution, this observation is in contrast with that reported for some heteronuclear Group IB metal clusters that undergo intramolecular molecular core rearangements in solution [9].

TABLE 1. Selected bond lengths (Å) and angles (°) in $[Os_8(CO)_{22}(Au_2dppb)]$ (**3**)

Os(1)–Os(2)	2.763(1)	Os(1)–Os(2)–Os(4)	63.71(3)	Os(1)–Os(6)–Os(7)	118.80(4)
Os(1)–Os(6)	2.790(2)	Os(6)–Os(2)–Os(4)	63.67(3)	Au(1)–Os(6)–Os(8)	127.12(3)
Os(1)–Au(1)	2.907(1)	Os(7)–Os(2)–Os(4)	95.63(4)	Au(2)–Os(6)–Os(8)	61.90(4)
Os(1)–Os(4)	2.936(1)	Os(5)–Os(2)–Os(4)	63.64(4)	Os(2)–Os(6)–Os(8)	88.65(4)
Os(2)–Os(3)	2.720(1)	Os(2)–Os(3)–Os(7)	60.33(4)	Os(1)–Os(6)–Os(8)	123.96(4)
Os(2)–Os(6)	2.776(1)	Os(2)–Os(3)–Os(5)	59.79(3)	Os(7)–Os(6)–Os(8)	59.67(3)
Os(2)–Os(7)	2.791(2)	Os(7)–Os(3)–Os(5)	60.17(4)	Au(1)–Os(6)–Os(4)	96.82(4)
Os(2)–Os(5)	2.800(1)	Os(2)–Os(4)–Au(2)	114.31(4)	Au(2)–Os(6)–Os(4)	61.12(3)
Os(2)–Os(4)	2.800(1)	Os(2)–Os(4)–Os(1)	57.53(3)	Os(2)–Os(6)–Os(4)	58.56(3)
Os(3)–Os(7)	2.831(1)	Au(2)–Os(4)–Os(1)	87.70(4)	Os(1)–Os(6)–Os(4)	61.56(4)
Os(3)–Os(5)	2.889(1)	Os(2)–Os(4)–Os(6)	57.77(3)	Os(7)–Os(6)–Os(4)	91.57(4)
Os(4)–Au(2)	2.908(1)	Au(2)–Os(4)–Os(6)	56.56(3)	Os(8)–Os(6)–Os(4)	62.50(4)
Os(4)–Os(6)	2.941(1)	Os(1)–Os(4)–Os(6)	56.69(4)	Os(2)–Os(7)–Os(3)	57.87(3)
Os(4)–Os(5)	2.952(1)	Os(2)–Os(4)–Os(5)	58.18(3)	Os(2)–Os(7)–Os(6)	59.10(4)
Os(4)–Os(8)	3.044(2)	Au(2)–Os(4)–Os(5)	116.16(4)	Os(3)–Os(7)–Os(6)	116.82(5)
Os(5)–Os(7)	2.867(2)	Os(1)–Os(4)–Os(5)	115.64(3)	Os(2)–Os(7)–Os(5)	59.29(4)
Os(5)–Os(8)	2.875(1)	Os(6)–Os(4)–Os(5)	87.00(4)	Os(3)–Os(7)–Os(5)	60.92(3)
Os(6)–Au(1)	2.725(1)	Os(2)–Os(4)–Os(8)	85.91(4)	Os(6)–Os(7)–Os(5)	90.64(4)
Os(6)–Au(2)	2.772(1)	Au(2)–Os(4)–Os(8)	59.00(3)	Os(2)–Os(7)–Os(8)	89.53(4)
Os(6)–Os(7)	2.838(1)	Os(1)–Os(4)–Os(8)	115.11(4)	Os(3)–Os(7)–Os(8)	121.01(4)
Os(6)–Os(8)	2.926(1)	Os(6)–Os(4)–Os(8)	58.51(4)	Os(6)–Os(7)–Os(8)	61.70(3)
Os(7)–Os(8)	2.868(1)	Os(5)–Os(4)–Os(8)	57.27(3)	Os(5)–Os(7)–Os(8)	60.15(3)
Os(8)–Au(2)	2.933(1)	Os(2)–Os(5)–Os(7)	58.99(4)	Os(7)–Os(8)–Os(5)	59.91(3)
Au(1)–Au(2)	2.975(1)	Os(2)–Os(5)–Os(8)	89.23(4)	Os(7)–Os(8)–Os(6)	58.64(3)
Os(2)–Os(1)–Os(6)	59.99(4)	Os(7)–Os(5)–Os(8)	59.94(3)	Os(5)–Os(8)–Os(6)	88.75(4)
Os(2)–Os(1)–Au(1)	117.04(4)	Os(2)–Os(5)–Os(3)	57.11(4)	Os(7)–Os(8)–Au(2)	115.10(4)
Os(6)–Os(1)–Au(1)	57.11(3)	Os(7)–Os(5)–Os(3)	58.91(3)	Os(5)–Os(8)–Au(2)	117.85(4)
Os(2)–Os(1)–Os(4)	58.76(3)	Os(8)–Os(5)–Os(3)	118.79(4)	Os(6)–Os(8)–Au(2)	56.46(3)
Os(6)–Os(1)–Os(4)	61.75(3)	Os(2)–Os(5)–Os(4)	58.18(3)	Os(7)–Os(8)–Os(4)	88.92(4)
Au(1)–Os(1)–Os(4)	93.06(4)	Os(7)–Os(5)–Os(4)	90.75(4)	Os(5)–Os(8)–Os(4)	59.77(3)
Os(3)–Os(2)–Os(1)	169.63(4)	Os(8)–Os(5)–Os(4)	62.96(4)	Os(6)–Os(8)–Os(4)	59.00(3)
Os(3)–Os(2)–Os(6)	122.91(5)	Os(3)–Os(5)–Os(4)	115.19(4)	Au(2)–Os(8)–Os(4)	58.20(3)
Os(1)–Os(2)–Os(6)	60.50(4)	Au(1)–Os(6)–Au(2)	65.52(3)	Os(6)–Au(1)–Os(1)	59.28(4)
Os(3)–Os(2)–Os(7)	61.79(4)	Au(1)–Os(6)–Os(2)	123.04(4)	Os(6)–Au(2)–Os(4)	62.32(3)
Os(1)–Os(2)–Os(7)	121.45(4)	Au(2)–Os(6)–Os(2)	119.65(4)	Os(6)–Au(2)–Os(8)	61.63(3)
Os(6)–Os(2)–Os(7)	61.29(3)	Au(1)–Os(6)–Os(1)	63.60(4)	Os(4)–Au(2)–Os(8)	62.80(4)
Os(3)–Os(2)–Os(5)	63.10(3)	Au(2)–Os(6)–Os(1)	93.43(4)	P(1)–Au(1)–Os(6)	161.92(14)
Os(1)–Os(2)–Os(5)	127.27(3)	Os(2)–Os(6)–Os(1)	59.51(3)	P(1)–Au(1)–Os(1)	136.15(13)
Os(6)–Os(2)–Os(5)	93.36(4)	Au(1)–Os(6)–Os(7)	171.15(4)	P(2)–Au(2)–Os(6)	160.0(2)
Os(7)–Os(2)–Os(5)	61.72(4)	Au(2)–Os(6)–Os(7)	121.57(4)	P(2)–Au(2)–Os(4)	136.21(13)
Os(3)–Os(2)–Os(4)	126.61(4)	Os(2)–Os(6)–Os(7)	59.61(4)	P(2)–Au(2)–Os(8)	128.9(2)

The molecular structure of **3** has been determined by a single crystal X-ray diffraction analysis (see Fig. 2). Selected bond lengths and angles are presented in Table 1. The central osmium core of the cluster consists of a bicapped octahedron, one of the gold atoms caps a face of this octahedron and the remaining gold atom bridges between one osmium of the octahedron and a capping osmium atom. The two golds also lie within close proximity to each other (2.975(1) Å) and hence there is the possibility of a significant bonding interaction between these two atoms, as occurs for a number of digold derivatives. The bicapped octahedral geometry of the osmium core is the identical geometry to that reported for the precursor cluster $[PPN]_2[Os_8(CO)_{22}]$. However in **3** the osmium–osmium distances observed within the central osmium core are on average 0.040 Å longer than those reported in $[PPN]_2[Os_8(CO)_{22}]$. This lengthening of metal–metal contacts is consistent with a decrease in electron density within the core due to the coordination of the gold atoms and the concomitant donation of electron density to the gold atoms. The largest increase in metal–metal distances is found for the face to which the gold atoms coordinate (defined by atoms Os(1), Os(4), Os(6) and Os(8)), with an average increase of 0.087 Å. In comparison with this observation, the osmium–osmium bond lengths in the opposite face of the cluster (defined by atoms Os(3), Os(5), Os(7) and Os(8)) show an average increase of only 0.026 Å compared to $[PPN]_2[Os_8(CO)_{22}]$. It is likely that the coordination of the gold atoms is via hybrid orbitals, directed at the midpoint of the Os(1)–Os(6) edge for Au(1) and at the centroid of the Os(4), Os(6), Os(8) face for Au(2). The P(1)–Au(1) and P(2)–Au(2) vectors make angles of 163.3 and 161.2° with the Os(1)–Os(6) midpoint and Os(4), Os(6), Os(8) centroid respectively, supporting this postulation. The atom Os(6) has the highest metal–metal connectivity, with five osmium–osmium bonds and two osmium–gold bonds, with these latter two bonds being the shortest of the osmium gold bonds observed (2.772(1), 2.725(1) Å). All carbonyl ligands in **5** are terminal, with this observation in contrast to that reported for $[PPN]_2[Os_8(CO)_{22}]$, where two bridging carbonyl groups are present [10]. The observed overall molecular geometry of **3** is in agreement with the spectroscopic data, which indicated that the two gold atoms occupied non-equivalent sites in the cluster and it is likely that the same geometry is indeed retained in solution. The cluster **3** has an electron count of 110, this is in agreement with that predicted from the polyhedral skeletal electron pair theory for condensed polyhedra [11].

From the spectroscopic data and the X-ray structural determination, it can be concluded that the addition of the di-gold fragments 'Au_2L^{2+}', occur with retention of the bicapped octahedral geometry of the Os_8 core. Whereas reaction with the mono-gold fragment '$AuPPh_3^+$', results in the formation of two isomers, one of which retains the bicapped octahердal geometry, however for the other isomer a major core rearrangement has occurred, with the former being the kinetically favoured product whereas the latter is the thermodynamically favoured isomer.

3. Experimental section

All reactions were performed under purified dinitrogen by standard Schlenk and vacuum line techniques [12]. Solvents used were distilled from appropiate drying agents under dinitrogen. Routine separations of products were performed by thin layer chromotography using commercially prepared glass plates, precoated to 0.25 mm thickness with Merck Kieselgel 60 PF_{254}, or using laboratory prepared glass plates coated to 1 mm thickness with Merck Kieselgel 60 PF_{254}.

TABLE 2. Spectroscopic and analytical data for compounds **1–5**

Compound	IR (ν CO, cm^{-1}, CH_2Cl_2)	MS (m/e) [a]	NMR (pppm, $CDCl_3$) ^{31}P	NMR (pppm, $CDCl_3$) ^1H
$[Os_8(CO)_{22}(Au_2dppm)]$(**1**)	2093 m, 2055 vs, 2044 vs 2024 m, 2010 m, 1995 w, 1975 w	2927 (2930)	54.1(d), 77.9(d)	3.27(q), 4.22(q) 7.14–7.74(m)
$[Os_8(CO)_{22}(Au_2dppe)]$(**2**)	2093 m, 2055 vs, 2043 vs 2024 m, 2010 m, 1995 w, 1978 w	2942 (2944)	67.3(s), 83.8(s)	2.55–3.23(m) 7.41–7.88(m)
$[Os_8(CO)_{22}(Au_2dppb)]$(**3**)	2093 m, 2056 vs, 2043 vs 2025 m, 2010 m, 1993 w, 1973 w	2970 (2972)	58.1(s), 86.1(s)	2.27–3.00(m) 7.41–7.81(m)
$[Os_8(CO)_{22}(AuPPh_3)_2]$(**4**)	2089 m, 2053 vs, 2045 vs, 2025 m, 2007 w, 1992 w, 1950 w	3067 (3070)	78.4(s)	7.26–7.74(m)
$[Os_8(CO)_{22}(AuPPh_3)_2]$(**5**)	2092 m, 2055 vs, 2042 vs, 2025 m, 2009 m, 1987 w, 1975 w	3067 (3070)	70.2(s), 89.9(s)	7.22–7.78(m)

[a] Calculated values in parentheses

IR spectra were recorded as dichloromethane solutions on a Perkin-Elmer 1710 Fourier Transform spectrometer. ^1H and $^{31}P\{^1H\}$ spectra were recorded on a Bruker AM-400 spectrometer and were referenced to external tetramethylsilane and 85% H_3PO_4 respectively. Mass spectral data were obtained by the method of Liquid Secondary Ion Mass Spectrometry (LSIMS) on a Kratos MS-50 mass spectrometer. Elemental analyses were performed in this department. The compounds [PPN]$_2$[Os$_8$(CO)$_{22}$], Au(PPh$_3$)NO$_3$ and Au$_2$Cl$_2$L (where L = dppm,dppe,dppb) were prepared according to literature procedures [13–15].

3.1. Preparation of [Os$_8$(CO)$_{22}$(AuPPh$_3$)$_2$]

To a solution of 50 mg (0.016 mmole) of [PPN]$_2$-[Os$_8$(CO)$_{22}$] was dissolved in 50 ml of dichloromethane was added a solution of 16 mg (0.032 mmole) Au(PPh$_3$)NO$_3$ in 20 ml of dichloromethane. The mixture was stirred at room temperature for 1 h, and the solvent was then removed *in vacuo*. Purification of the

TABLE 3. Fractional atomic coordinates equivalent isotropic displacement coefficients (Å^2) for [Os$_8$(CO)$_{22}$Au(PPh$_2$\{CH$_2$\}$_4$PPh$_2$)] (3)

	x	y	z	U_{eq}		x	y	z	U_{eq}
Os(1)	0.10647(4)	0.05101(5)	0.28506(5)	0.0256(2)	C(41)	0.099(2)	0.297(2)	0.134(2)	0.062(7)
Os(2)	0.08924(4)	0.19346(5)	0.42301(5)	0.0248(2)	C(42)	0.115(1)	0.137(2)	0.108(2)	0.039(5)
Os(3)	0.06673(5)	0.31248(6)	0.58048(6)	0.0339(2)	C(43)	−0.020(1)	0.175(1)	0.180(2)	0.032(4)
Os(4)	0.11103(4)	0.22161(5)	0.22983(5)	0.0249(2)	C(51)	0.106(2)	0.436(2)	0.298(2)	0.050(5)
Os(5)	0.10032(5)	0.36565(5)	0.39620(6)	0.0286(2)	C(52)	0.112(2)	0.474(2)	0.491(2)	0.057(6)
Os(6)	0.26066(4)	0.20360(5)	0.40181(5)	0.0225(2)	C(53)	−0.033(1)	0.322(2)	0.338(2)	0.037(4)
Os(7)	0.24365(5)	0.33950(5)	0.55878(5)	0.0277(2)	C(61)	0.284(2)	0.144(2)	0.507(2)	0.048(5)
Os(8)	0.27844(4)	0.38403(5)	0.37250(6)	0.0271(2)	C(62)	0.391(1)	0.225(2)	0.424(2)	0.033(4)
Au(1)	0.29098(4)	0.06542(5)	0.27749(6)	0.0301(2)	C(71)	0.250(2)	0.277(2)	0.666(2)	0.049(5)
Au(2)	0.29449(4)	0.23670(5)	0.21783(5)	0.0288(2)	C(72)	0.272(1)	0.456(2)	0.654(2)	0.043(5)
P(1)	0.3615(3)	−0.0314(4)	0.2140(4)	0.035(1)	C(73)	0.375(1)	0.362(2)	0.590(2)	0.042(5)
P(2)	0.3634(3)	0.2449(4)	0.0877(4)	0.032(1)	C(81)	0.275(1)	0.429(2)	0.252(2)	0.048(5)
O(11)	0.101(1)	−0.084(1)	0.086(1)	0.060(4)	C(82)	0.405(2)	0.401(2)	0.388(2)	0.046(5)
O(12)	0.134(1)	−0.085(1)	0.410(2)	0.071(5)	C(83)	0.303(1)	0.504(2)	0.454(2)	0.038(4)
O(13)	−0.100(1)	−0.045(1)	0.207(1)	0.042(3)	C(1)	0.303(1)	0.147(1)	−0.034(1)	0.027(4)
O(21)	0.093(1)	0.070(1)	0.571(1)	0.056(4)	C(2)	0.285(1)	0.057(2)	−0.010(2)	0.041(5)
O(22)	−0.120(1)	0.113(1)	0.354(1)	0.048(4)	C(3)	0.369(1)	0.028(2)	0.030(2)	0.041(5)
O(31)	0.062(1)	0.214(1)	0.753(1)	0.064(5)	C(4)	0.343(1)	−0.057(2)	0.070(2)	0.041(5)
O(32)	−0.140(1)	0.272(1)	0.520(1)	0.062(4)	C(111)	0.330(2)	−0.144(2)	0.235(2)	0.047(5)
O(33)	0.092(1)	0.488(2)	0.739(2)	0.075(5)	C(112)	0.398(2)	−0.183(3)	0.274(3)	0.088(9)
O(41)	0.085(1)	0.327(2)	0.062(2)	0.082(6)	C(113)	0.366(3)	−0.273(4)	0.286(4)	0.13(2)
O(42)	0.102(1)	0.090(1)	0.025(1)	0.042(3)	C(114)	0.276(3)	−0.312(3)	0.261(3)	0.11(1)
O(43)	−0.098(1)	0.147(1)	0.146(1)	0.045(4)	C(115)	0.211(3)	−0.271(4)	0.241(4)	0.13(2)
O(51)	0.097(1)	0.484(2)	0.242(2)	0.080(6)	C(116)	0.239(3)	−0.190(3)	0.216(3)	0.12(1)
O(52)	0.119(1)	0.548(1)	0.543(1)	0.064(5)	C(121)	0.487(1)	0.012(2)	0.280(2)	0.036(4)
O(53)	−0.109(1)	0.301(1)	0.306(1)	0.062(4)	C(122)	0.545(2)	−0.007(2)	0.225(2)	0.058(6)
O(61)	0.303(1)	0.107(1)	0.576(1)	0.065(5)	C(123)	0.642(2)	0.030(2)	0.282(2)	0.066(7)
O(62)	0.467(1)	0.244(1)	0.454(1)	0.041(3)	C(124)	0.674(2)	0.079(2)	0.386(2)	0.056(6)
O(71)	0.264(1)	0.243(1)	0.735(1)	0.058(4)	C(125)	0.616(2)	0.092(2)	0.438(2)	0.066(7)
O(72)	0.295(1)	0.523(1)	0.721(1)	0.067(5)	C(126)	0.520(1)	0.062(2)	0.385(2)	0.042(5)
O(73)	0.452(1)	0.383(1)	0.624(1)	0.055(4)	C(211)	0.486(1)	0.256(2)	0.122(2)	0.041(5)
O(81)	0.270(1)	0.464(1)	0.184(1)	0.063(4)	C(212)	0.528(2)	0.262(2)	0.044(2)	0.054(6)
O(82)	0.482(1)	0.422(1)	0.403(1)	0.059(4)	C(213)	0.618(2)	0.263(2)	0.068(2)	0.068(7)
O(83)	0.323(1)	0.576(1)	0.506(1)	0.055(4)	C(214)	0.663(2)	0.261(2)	0.166(2)	0.080(8)
C(11)	0.109(1)	−0.030(2)	0.162(2)	0.038(4)	C(215)	0.625(2)	0.257(2)	0.248(2)	0.066(7)
C(12)	0.127(1)	−0.032(2)	0.363(2)	0.039(5)	C(216)	0.533(2)	0.259(2)	0.225(2)	0.057(6)
C(13)	−0.022(1)	−0.006(1)	0.238(1)	0.030(4)	C(221)	0.360(1)	0.343(2)	0.042(2)	0.045(5)
C(21)	0.092(1)	0.120(1)	0.516(1)	0.031(4)	C(222)	0.432(2)	0.426(2)	0.096(2)	0.060(6)
C(22)	−0.042(1)	0.147(1)	0.376(1)	0.025(4)	C(223)	0.420(2)	0.504(3)	0.061(3)	0.088(9)
C(31)	0.061(1)	0.255(2)	0.688(2)	0.041(5)	C(224)	0.347(2)	0.499(3)	−0.013(3)	0.085(9)
C(32)	−0.063(1)	0.289(2)	0.540(2)	0.043(5)	C(225)	0.277(2)	0.431(3)	−0.055(3)	0.086(9)
C(33)	0.086(1)	0.420(2)	0.681(2)	0.045(5)	C(226)	0.279(2)	0.345(2)	−0.032(2)	0.079(8)

residue by TLC using a 45% dichloromethane/hexane mixture as eluent afforded two major products. On the basis of IR and NMR spectroscopic data the two products were characterised as the isomers of [$Os_8(CO)_{22}(AuPPh_3)_2$] (**4** and **5**), and were obtained in approximately 60% and 25% yield respectively. The spectroscopic data for these compounds are summarised in Table 2. [Found: (**5**) C, 22.73; H, 0.96; Calculated for $Os_8Au_2P_2O_{22}C_{58}H_{30}$ (**5**): C, 22.78; H, 0.98%]

3.2. Preparation of [$Os_8(CO)_{22}(Au_2L)$]{where L = dppm (1), dppe(2), dppb(3)}

To a solution of 50 mg (0.016 mmole) of [PPN]$_2$[$Os_8(CO)_{22}$] in 50 ml of dichloromethane were added one equivalent (0.016 mmole) of Au_2Cl_2L and an excess of the halide abstractor $TlPF_6$. The mixture was stirred at room temperature for 2 h and the solvent was then removed *in vacuo*. Purification of the residue by TLC using a 60% dichloromethane/hexane mixture as eluent afforded the product [$Os_8(CO)_{22}(Au_2L)$] in almost quantitative yield. The formulations of these compounds were based on the spectroscopic data which are summarised in Table 2. [Found: (**1**) C, 19.37; H, 0.77; Calculated for $Os_8Au_2P_2O_{22}C_{47}H_{22}$ (**1**): C, 19.36; H, 0.76%; Found: (**2**) C, 19.82; H, 0.81; P, 2.36; Calculated for $Os_8Au_2P_2O_{22}C_{48}H_{24}$ (**2**): C, 19.68; H, 0.83; P, 2.11%; Found: (**3**) C, 20.30; H, 0.89; P, 2.26; Calculated for $Os_8Au_2P_2O_{22}C_{50}H_{28}$ (**3**): C, 20.30; H, 0.95; P, 2.09%;]

3.3. Crystal structure determination for [$Os_8(CO)_{22}(Au_2dppb)$] (3)

$Os_8Au_2P_2O_{22}C_{50}H_{28}$, triclinic, space group $P\bar{1}$, $a = 15.859(3)$, $b = 15.925(3)$, $c = 13.376(3)$ Å, $\alpha = 100.90(3)$, $\beta = 105.69(3)$, $\gamma = 104.81(3)°$, $U = 3021(1)$ Å^3, $Z = 2$, $F(000) = 2600$, μ(Mo K$_\alpha$) = 21.711 mm^{-1}, $D_c = 3.252$ g cm^{-3}. A brown block shaped crystal of approximate dimensions 0.40 × 0.40 × 0.40 mm was mounted on a glass fibre, D_m not recorded, accurate lattice parameters determined from 25 reflections ($\theta = 13.10$–$14.94°$). Intensity data were measured on a Rigaku AFC7R diffractometer using monochromated Mo K$_\alpha$ radiation and ω scan mode to a maximum value for θ of 25.0°. Three standard reflections were monitored after every 100 reflections collected and showed no significant decrease in standard intensity during the data collection time. A total of 7901 reflections were measured within the range $0 \leq h \leq 18$, $-14 \leq k \leq 18$, $-15 \leq l \leq 14$ and averaged to yield 7888 unique reflections ($R_{int} = 0.0450$) of which 6202 were judged as significant by the criterion that $F_{obs} > 4\sigma(F_{obs})$. Corrections for Lorentz and polarisation effects were applied. Absorption corrections was applied using the method of Stuart and Walker [16], minimum and maximum correction, 0.477 and 1.758 respectively. Structure solution was by a combination of direct methods and Fourier techniques. Full matrix least-squares refinement on F^2_{obs} for 7888 data and 397 parameters converged to $wR2 = 0.1592$ (all data), conventional $R = 0.0529$ (observed data), $(\Delta/\sigma)_{max} = -0.004$, GOF (all data) = 1.058. The function minimised was $\Sigma w(F^2_{obs} - F^2_{calc})^2$, $w = 1/[\sigma^2(F^2_{obs}) + (0.0976P)^2 + 42.1901P]$ where $P = (F^2_{obs} + 2F^2_{calc})/3$ and σ was obtained from counting statistics. A final difference electron density Fourier synthesis revealed maximum and minimum residual electron density peaks of 3.523 and -3.038 eÅ^{-3} which were located within close proximity of osmium atoms. For all calculations the teXsan, SHELX-86 and SHELX-93 program packages were used [17–19]. Fractional atomic coordinates are listed in Table 3. Additional information comprising hydrogen atom coordinates, anisotropic thermal parameters and full listings of bond lengths and angles has been deposited at the Cambridge Crystallographic Data Centre.

Acknowledgements

We gratefully acknowledge the S.E.R.C. (S.L.I.), Cambridge Commonwealth Trust and the U.K. Committee of Vice Chancellors and Principals (Z.A.) for financial support.

References

1 S.L. Ingham, J. Lewis and P.R. Raithby, *J. Chem. Soc., Chem. Commun.*, (1993) 166.
2 E. Charalambous, L.H. Gade, B.F.G. Johnson, J. Lewis, M. McPartlin and H. Powell, *J. Chem. Soc., Chem. Commun.*, (1990) 688.
3 A.J. Amoroso, L.H. Gade, B.F.G. Johnson, J. Lewis, P.R. Raithby and W.-T. Wong, *Angew. Chem., Int. Ed. Engl., 30* (1991) 107.
4 B.F.G. Johnson, J. Lewis, W.J.H. Nelson, M.D. Vargas, D. Braga, K. Henrick and M. McPartlin, *J. Chem. Soc., Dalton Trans.*, (1986) 975.
5 V. Dearing, S.R. Drake, B.F.G. Johnson, J. Lewis, M. McPartlin and H.R. Powell, *J. Chem. Soc., Chem. Commun.*, (1988) 1331.
6 L.H. Gade, B.F.G. Johnson, J. Lewis, M. McPartlin and H.R. Powell, *J. Chem. Soc., Chem. Commun.*, (1992) 921.
7 E. Charalambous, L.H. Gade, B.F.G. Johnson, T. Kotch, A.J. Lees, J. Lewis and M. McPartlin, *Angew. Chem., Int. Ed. Engl., 29* (1990) 1137.
8 B.F.G. Johnson, J. Lewis, W.J.H. Nelson, P.R. Raithby and M.D. Vargas, *J. Chem. Soc., Chem. Commun.*, (1983) 608.
9 I.D. Salter, *Adv. Organomet. Chem., 29* (1989) 249.
10 P.F. Jackson, B.F.G. Johnson, J. Lewis and P.R. Raithby, *J. Chem. Soc., Chem. Commun.*, (1980) 60.
11 D.M.P. Mingos, *J. Chem. Soc., Chem. Commun.*, (1983) 706.
12 D.F. Shriver, *Manipulation of air-sensitive compounds*, McGraw-Hill, New York, 1969.

13 D. Braga, K. Henrick, B.F.G. Johnson, J. Lewis, M. McPartlin, W.J.H. Nelson and M. D. Vargas, *J. Chem. Soc., Chem. Commun.*, (1982) 419.

14 A.M. Mueting, B.D. Alexander, P.D. Bole, A.L. Casalnuovo, L.N. Itp, B.J. Johnson and L.H. Pignolet, *Inorg. Synth.*, *29* (1992) 280.

15 S.J. Berners-Price, M.A. Mazid and P.J. Sadler, *J. Chem. Soc., Dalton Trans.*, (1984) 969.

16 N. Walker and D. Stuart, *Acta Crystallogr., Sect. A*, *39* (1983) 158.

17 teXsan: Single Crystal Structure Analysis Software, Version 1.6, 1993, Molecular Structure Corporation, The Woodlands, TX 77381, USA.

18 G.M. Sheldrick, *Acta Crystallogr., Sect. A.*, *46* (1993) 467.

19 G.M. Sheldrick, *J. Appl. Cryst.*, in preparation.